Analytical Methods

www.rsc.org/methods

Volume 5 | Number 22 | 21 November 2013 | Pages 6249–6540

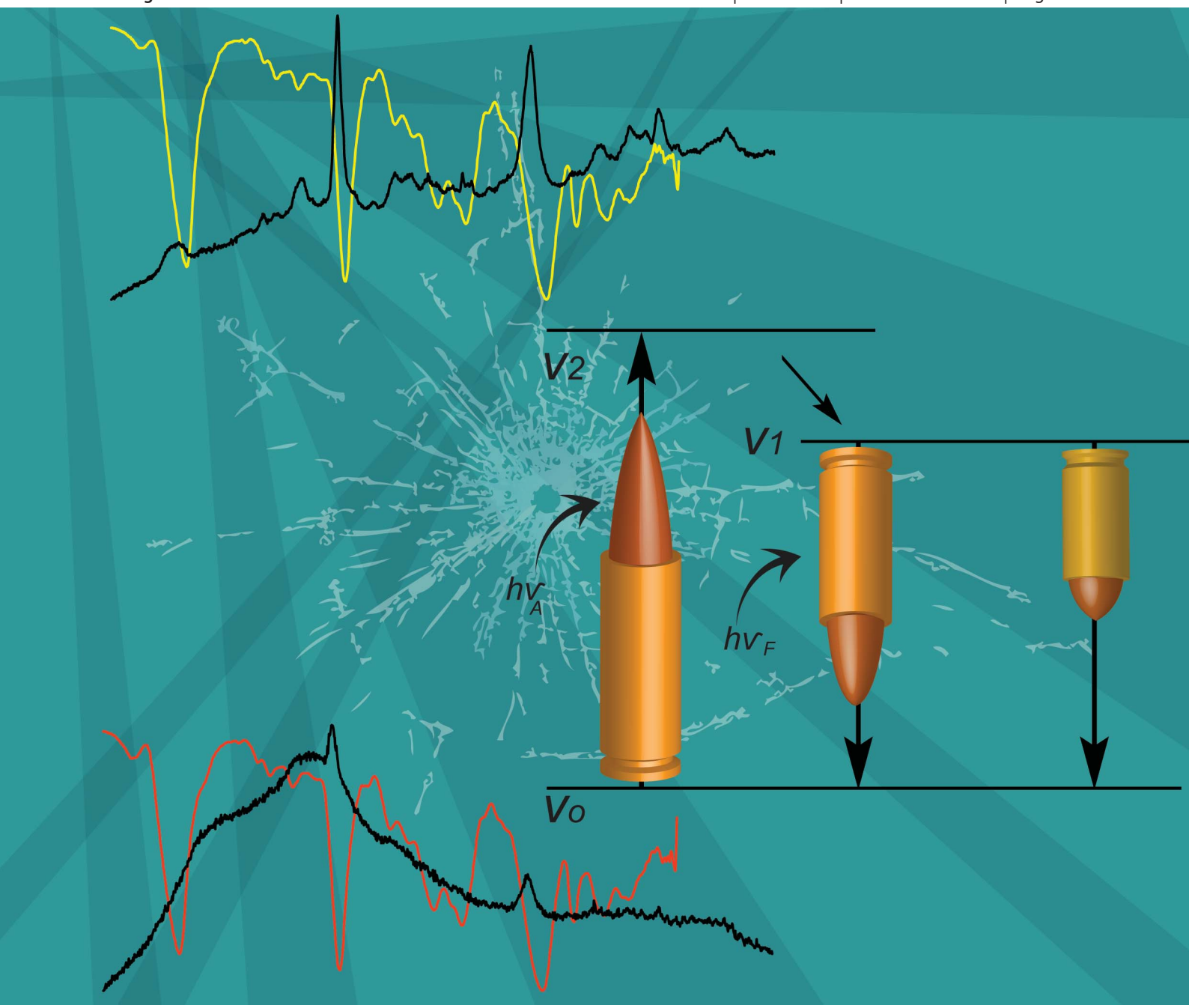

ISSN 1759-9660

RSC Publishing

PAPER

Bueno and Lednev

Advanced statistical analysis and discrimination of gunshot residue implementing combined Raman and FT-IR data

1759-9660(2013)5:22;1-J

Analytical Methods

RSC Publishing

PAPER

View Article Online
View Journal | View Issue

Cite this: *Anal. Methods*, 2013, **5**, 6292

Advanced statistical analysis and discrimination of gunshot residue implementing combined Raman and FT-IR data†

Justin Bueno and Igor K. Lednev*

Received 1st May 2013
Accepted 22nd August 2013

DOI: 10.1039/c3ay40721g

www.rsc.org/methods

We report a novel analytical and statistical approach to gunshot residue (GSR) analysis, characterization and discrimination. Spectroscopic data from two complementary techniques (Raman and FT-IR) were combined into a single dataset to improve statistical discrimination of GSR.

Gunshot residue (GSR) consists of the burnt and partially burnt by-products expelled during a firearm discharge. The firearm, cartridge case, ammunition propellant and primer all contribute to the chemical composition of GSR. Currently, GSR detection offers limited forensic information. The major forensic conclusion is that GSR detected on suspects confirms that they discharged a firearm, or were in the vicinity of a discharging firearm. Recently, GSR analysis has begun targeting the elucidation of forensically relevant parameters (*e.g.*, firearm, ammunition or caliber size). Evidentiary analysis of GSR in this manner offers several obvious advantages over current ballistics methods. Most importantly, when a firearm is discharged, hundreds of GSR particles are distributed to numerous locations around the crime scene. The probability of recovering GSR particles is therefore much greater than recovering other types of ballistics evidence (*e.g.*, bullet, cartridge case or firearm).

Several different spectroscopic and analytical techniques have been utilized for the analysis and characterization of GSR. Scanning electron microscopy coupled with energy dispersive X-ray spectroscopy (SEM-EDS/X) is the most widely accepted tool for GSR analysis.[1] The method has been applied to investigate the impact of certain forensically relevant parameters on the chemical composition of the resulting GSR. Specifically, the impact of ammunition type and brand on GSR was investigated.[2–4] The impact of propellant type and projectile (bullet) composition on the resulting GSR was also investigated using high-performance liquid chromatography (HPLC) and inductively coupled plasma-mass spectrometry (ICP-MS).[5,6]

López-López *et al.* visually discriminated the Raman spectra of GSR particles originating from different ammunition propellants.[7] Specific chemical markers that are characteristic of ammunition propellants were detected in the resulting GSR, generating a link between the GSR samples and particular ammunition. We have recently reported the use of chemometric analyses of Raman[8] and attenuated total reflectance Fourier transform infrared (ATR-FT-IR)[9] spectroscopic data, to discriminate GSR samples originating from different firearm–ammunition combinations. These studies investigated a link between firearm caliber (a crucial investigative parameter) and the spectroscopic characteristics of GSR. Additionally, Cetó *et al.* differentiated GSR samples collected from suspects with various involvements in a mock shooting incident *via* electrochemical analysis.[10]

Hogg *et al.* recently reported the use of SEM-EDS in the identification of GSR originating from heavy-metal free ammunition.[11] The study was able to identify GSR without detecting heavy metals that are considered "characteristic" of GSR. Furthermore, multivariate analysis was implemented to differentiate GSR samples among six different brands of heavy-metal free ammunition. An alternative approach to GSR elemental analysis and characterization was proposed by Abrego *et al.* The use of ICP-MS for elemental analysis of GSR was found to reduce analysis time significantly.[12] Steffen *et al.* applied both EDS and ICP-MS analysis, to differentiate GSR particles originating from ammunition primers with varying chemical compositions.[13] ICP-MS isotope ratio measurements were found to be an additional parameter by which GSR from lead-containing primers could be differentiated.

Although numerous studies have applied different analytical techniques to GSR analysis, to our knowledge no study has combined the experimental spectra from any two methods into a single dataset. Because Raman and infrared spectroscopies often obey different selection rules and provide complementary information, combining the two could permit a greater amount of spectroscopic information to be extracted from each sample. As a result, an increase in sensitivity/specificity for discriminant analysis (chemometrics) can be expected, due to the new dimensions added to the dataset. Here, we report the

Department of Chemistry, University at Albany, State University of New York, 1400 Washington Avenue, Albany, New York 12222, USA. E-mail: ilednev@albany.edu; Fax: +1 (518) 442-3462; Tel: +1 (518) 591-886

† Electronic supplementary information (ESI) available. See DOI: 10.1039/c3ay40721g

application of such an approach for GSR analysis and characterization. The combined vibrational information was treated with exploratory and classification statistical analyses to discriminate GSR originating from different firearm–ammunition combinations.

Individual GSR particles were analyzed with confocal Raman microspectroscopy and ATR-FT-IR spectroscopy. Each of these spectroscopic methods offers several advantages over the current GSR identification techniques. An important advantage inherent to both techniques is that they do not depend on detecting heavy metals that are considered "characteristic" of GSR particles. The most prominent GSR identification techniques are dependent upon the detection of elemental lead, barium and antimony. As previously reported, Raman spectroscopy was able to detect both organic and inorganic components of GSR.[8] Furthermore, confocal Raman microspectroscopy offers non-contact rapid analysis. In contrast to Raman spectroscopy, ATR-FT-IR is not subject to fluorescence interference.

In this study, 46 randomly selected GSR particles were first analyzed individually by Raman spectroscopy. Twenty-four GSR particles originated from a 9 mm caliber firearm discharge, while the remaining 22 particles originated from a 0.38 inch (in.) caliber firearm. All particles were characterized using a Renishaw inVia confocal Raman microscope with a 785 nm excitation and a 50× objective. A single Raman spectrum was collected from each particle. GSR sample collection and ballistics information have been described previously.[8] All particles were stored in labeled containers and were subsequently analyzed using a PerkinElmer Spectrum 100 FT-IR spectrometer with an attached universal ATR sampling accessory. Thus, 92 total spectra were collected from 46 GSR particles.

Example raw Raman and FT-IR spectra (blue and red traces respectively) collected from the same GSR particle are illustrated in Fig. 1. Both spectra contain 14 bands over a range of approximately 1000 cm^{-1}. However, a majority of the bands in the Raman spectra experienced a shift compared to the FT-IR spectra. The difference in peak location varies from band to band (Table 1). Because all peak positions do not vary by the same wavenumbers, the variations are not caused by the calibration of the spectrometers. Therefore, the analyte could be responsible for these variations.

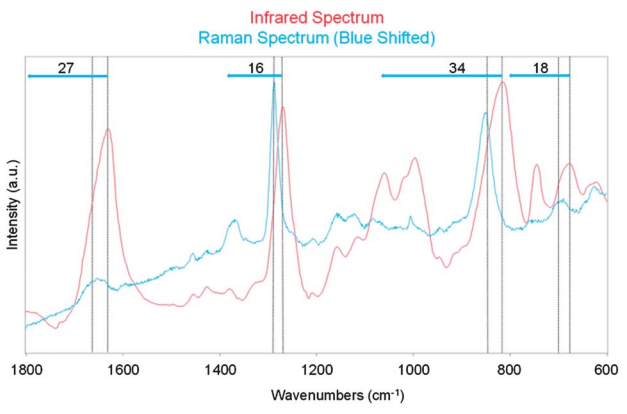

Fig. 1 Raw Raman and infrared (blue and red traces, respectively) spectra collected from the same "0.38 in." GSR particle. The FT-IR spectrum was transformed from transmittance to absorbance. Blue arrows indicate the intensity of the Raman peak shifts, for major vibrational modes.

Table 1 Peak positions for Raman and FT-IR spectra shown in Fig. 1. For the Raman spectrum, 12 out of 14 peaks experience an increase in wavenumbers, ranging from 34 to 1, as compared to FT-IR

Location of Raman band (cm^{-1})	Location of IR band (cm^{-1})	Difference (cm^{-1})
1657	1630	27
1455	1454	1
1427	1426	1
1370	1379	+9
1286	1270	16
1209	1210	+1
1158	1156	2
1121	1116	5
1084	1059	25
1005	996	9
849	815	34
763	754	18
695	677	18
628	620	8

The spectroscopic data of GSR was found to have a large contribution of nitrate ester explosives (R–O–NO_2 containing molecules). Nitrate esters such as nitrocellulose (NC), nitroglycerin (NG) and pentaerythritol tetranitrate (PETN) are commonly used as fuels in smokeless ammunition propellants.[14,15] The burnt and partially burnt residues of these molecules are common to organic GSR.[16] Symmetric and asymmetric stretching of the NO_2 group was assigned to the Raman bands at 1286 and 1657 cm^{-1}, respectively. These frequencies are characteristic of PETN.[17] The same modes were assigned to the infrared bands at 1270 and 1630 cm^{-1}.[18] PETN and other nitrate esters are highly symmetrical molecules, and the molecular point symmetry of PETN is S4.[19] We believe that the individual analytical techniques are probing different vibrational modes. Due to the rule of mutual exclusion and the symmetry of the analyte, these vibrational modes may not be both Raman and infrared active. The symmetry of the analyte could account for the observed peak shifts.

The Raman and FT-IR datasets were preprocessed separately. All spectral processing was performed using MATLAB 7.9.0 with the PLS toolbox. Raman spectra were subjected to cosmic ray removal, spectral smoothing, 6^{th} order polynomial baseline correction and normalization by area. The contribution of air was removed from all FT-IR spectra. Additionally, FT-IR spectra were transformed from transmittance to absorbance, log(1/T), and subjected to the same baseline correction and normalization treatment applied to the Raman spectra. Consequently, the area under all experimental spectra was equal.

The 92 total preprocessed Raman and FT-IR spectra were combined into 46 spectra, generating a "combined Raman-FT-IR" spectrum for each GSR particle. While the preprocessed Raman dataset was open in the MATLAB workspace, the FT-IR dataset was loaded, augmenting each Raman spectrum with its

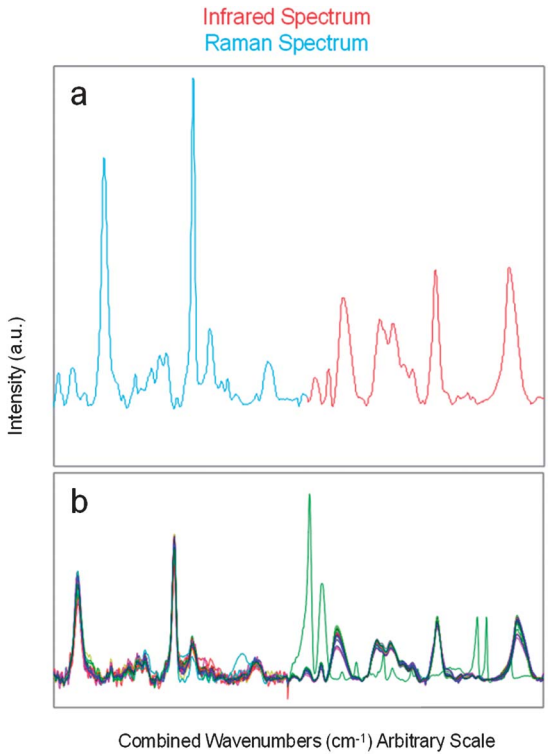

Fig. 2 (a) Individual baseline corrected spectra from Fig. 1, as a "combined Raman-FT-IR" spectrum. (b) Entire dataset of 46 "combined" spectra, including outliers (*i.e.* green trace).

corresponding FT-IR spectrum for each GSR particle. Fig. 2a illustrates a Raman spectrum (blue trace) augmented with the FT-IR spectrum (red trace) from the same GSR particle. To the best of our knowledge, this is the first report of the combination of Raman and FT-IR data from the same analyte for statistical purposes. Recently, Raman and fibre-optic reflectance spectra originating from the same samples were combined to enhance discrimination of medieval paint mixtures.[20] The dataset of 46 "combined spectra" (Fig. 2b) was subjected to mean centering for statistical analysis (not shown). Alternate data processing was performed, in which the experimental spectra from each method were subjected to mean centering before being combined. The absolute total area under the curves (sum of all 46 spectra) was only approximately 9% greater for the Raman spectra than for the infrared spectra after individual mean centering. We therefore conclude that the spectral contribution of each analytical method in the "combined spectra" was similar.

However, each analytical method (Raman and infrared) was observed to have a different statistical impact on the chemometric model. Fig. 3a represents the first principal component (PC) describing the exploratory data analysis. The vertical line is the demarcation between the Raman and infrared contributions (left and right side respectively) to the statistical model. The Raman contribution is mostly noise, while the infrared portion is represented by a spectral contribution. This divergence was attributed to a higher degree of variability observed in the FT-IR dataset. The statistical model could be described by

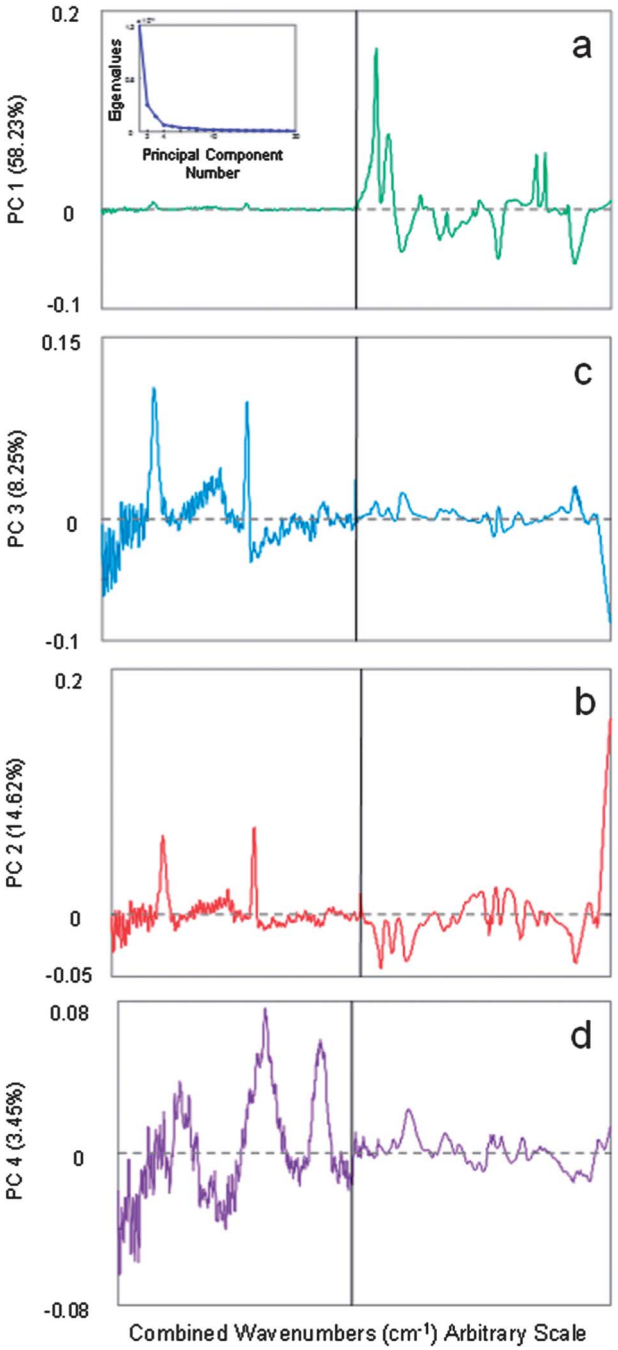

Fig. 3 (a) First principal component (PC) describing ~58% of the dataset for exploratory analysis. The vertical line represents the threshold for the contribution of the Raman and FT-IR datasets (left and right side respectively). Upper left inset shows the eigenvalues (scree) plot, used to determine the number of meaningful PCs which describe the dataset. (b–d) Subsequent meaningful PCs (second through forth).

four meaningful PCs (determined by the scree plot local minimum, Fig. 3a upper left insert). The ratio of spectral contribution (signal) to noise (*S*/*N*), comparing the Raman dataset to the infrared dataset, was found to vary over all PCs. Although subsequent PCs had a diminished impact on the statistical model, the second through fourth components illustrated an increase in the spectral contribution for the

Raman dataset (Fig. 3b–d), as compared to the first PC. Emphasizing that the two techniques provide complementary information is important for statistical analyses, for two reasons. First, a more encompassing statistical description is provided for each GSR particle due to the enhancement in extracted vibrational and statistical information. Second, we believe that the observed vibrational and statistical variations in the dataset originate from chemical variations between the two non-equivalent GSR samples. This observation directly correlates with the enhancement of any potential statistical discrimination.

The combined dataset was subjected to classification analysis. "Combined" spectra with high Q residual and/or hotelling T^2 values (values that determine the statistical limits of the dataset) reported during exploratory data analysis were identified as outliers and were removed from the dataset.[21] Partial least squares discriminant analysis (PLSDA) targeted the discrimination of GSR based on the firearm–ammunition combination or, more specifically, firearm caliber. Each combined spectrum was labeled (9 mm or 0.38 in.) prior to classification analysis. Results are reported through the supervised classification of all experimental spectra as being collected from a GSR particle, originating from a specific firearm–ammunition combination.

Comparisons of the PLSDA loadings (latent variables or LVs) to the PCs from Fig. 3, are illustrated in Fig. S1 ESI.† Four LVs were utilized to describe the dataset determined by scree plot minimum. Results from the first loadings of each statistical model (PCA and PLSDA) are very similar. However, the Raman contribution in LV 1 is slightly larger as compared to PC 1. The two features which increase in contribution from PCA to PLSDA correspond to the symmetric and asymmetric stretching of the NO_2 functional group, inherent to organic GSR.

Fig. 4a and b (initial and cross validated results, respectively) illustrate the resulting score plots. The red triangle and green star data points are "combined" spectra originating from the 0.38 in. and 9 mm firearm discharges respectively. The *x*-axis plots an individual "combined" spectrum of GSR. The *y*-axis is the probability that a spectrum will be assigned as originating from the 0.38 in. firearm discharge. The red dotted line denotes the "threshold" for classification as originating from the 0.38 in. caliber discharge.

The results report sensitivity/specificity rates of 100% for the combined approach. All spectroscopic data collected from the 0.38 in. caliber discharges were correctly assigned. Additionally, no false positive assignments were made because none of the 9 mm "combined" spectra were assigned as originating from the 0.38 in. sample. The initial classification was supported by the internal validation of the dataset through leave-one-out cross validation (Fig. 4b). Fig. 4b illustrates that cross validation increases the variation within the 9 mm dataset. However, the results are reproduced from the initial statistical model, suggesting that the dataset is stable.

The purpose of this study was to improve the sensitivity and specificity of the GSR discrimination method by combining data obtained using two complementary analytical methods, Raman and infrared spectroscopies. The results described here

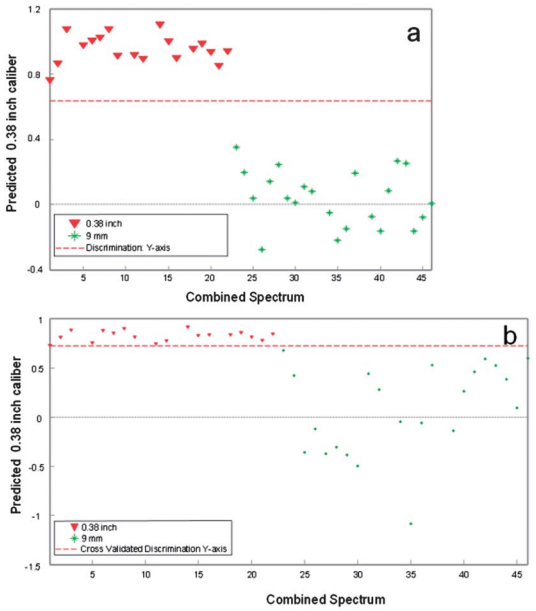

Fig. 4 (a) PLSDA of the combined dataset. Each data point represents a combined spectrum. Green stars and red triangles for GSR particles originating from 9 mm and 0.38 in. caliber discharges, respectively. The red dotted line is the threshold for assigning the combined spectrum as originating from the 0.38 in. discharge. (b) PLSDA classification with leave-one-out (LOO) cross-validation.

illustrate an improvement on our previously reported rates of classification. The lowest reported sensitivity/specificity for the exclusive Raman method was 98%, and the lowest cross-validated results for the exclusive FT-IR method were a sensitivity of 94% and specificity of 97%. It is important to note that although a smaller dataset was utilized (only 46 "combined" spectra), the combined method increased sensitivity and specificity results over the previously tested techniques.

Conclusions

Spectra from two different analytical techniques, *i.e.*, FT-IR and Raman spectroscopies, were combined into one dataset for statistical treatment. The two analytical methods provided complementary information. Due to their individual selection rules and the observed peak shifts in the experimental data (Fig. 1), the techniques appear to be probing different vibrational modes. These variations accounted for different statistical impacts on the dataset (Fig. 3). We believe that the vibrational and statistical variations were not uniform from sample to sample.

The hypothesis was tested by analyzing the dataset of "combined spectra" from GSR particles originating from 9 mm and 0.38 in. caliber discharges. The results illustrate the robustness of the combined approach. An increase in the sensitivity/specificity for the statistical discrimination was observed, compared to our previously reported individual methods. The method targets the discrimination of non-equivalent GSR samples. The simplest application of this research to a forensic investigator is in the comparison of a crime scene GSR sample to a GSR sample generated from recovered ballistics

evidence. Therefore, this approach could allow a firearms investigator to rule out a particular firearm–ammunition combination for generating a crime scene GSR sample.

Acknowledgements

We are grateful to Dr Barry Duceman, Director of Biological Science, New York State Police Forensic Investigation Center for continuous support, and Lieutenant Heller and Sergeant D'Allaird for providing the GSR samples. We also thank Kyle C. Doty for assistance with manuscript editing.

Notes and references

1 A. J. Schwoeble and D. L. Exline, *Current Methods in Forensic Gunshot Residue Analysis*, CRC Press, New York, 2000.
2 Z. Brozek-Mucha and A. Jankowicz, *Forensic Sci. Int.*, 2001, **123**, 39–47.
3 Z. Oommen and S. M. Pierce, *J. Forensic Sci.*, 2006, **51**, 509–519.
4 A. Martiny, A. P. C. Campos, M. S. Sader and M. A. L. Pinto, *Forensic Sci. Int.*, 2008, **177**, E9–E17.
5 W. A. MacCrehan, E. R. Patierno, D. L. Duewer and M. R. Reardon, *J. Forensic Sci.*, 2001, **46**, 57–62.
6 R. N. Udey, B. C. Hunter and R. W. Smith, *J. Forensic Sci.*, 2011, **56**, 1268–1276.
7 M. López-López, J. J. Delgado and C. García-Ruiz, *Anal. Chem.*, 2012, **84**, 3581–3585.
8 J. Bueno, V. Sikirzhytski and I. K. Lednev, *Anal. Chem.*, 2012, **84**, 4334–4339.
9 J. Bueno, V. Sikirzhytski and I. K. Lednev, *Anal. Chem.*, 2013, **85**, 7287–7294.
10 X. Cetó, A. M. O'Mahony, I. A. Samek, J. R. Windmiller, M. del Valle and J. Wang, *Anal. Chem.*, 2012, **84**, 10306–10314.
11 S. R. Hogg, B. C. Hunter and R. W. Smith, *Analysis of Lead-Free Ammunition by Scanning Electron Microscopy Using Energy Dispersive X-Ray Spectroscopy and Discrimination of Samples Using Multivariate Statistical Methods*, AAFS Annual Meeting, Washington, D.C., 2013.
12 Z. Abrego, A. Ugarte, N. Unceta, A. Fernández-Isla, M. A. Goicolea and R. J. Barrio, *Anal. Chem.*, 2012, **84**, 2402–2409.
13 S. Steffen, M. Otto, L. Niewoehner, M. Barth, Z. Brozek-Mucha, J. Blegstraaten and R. Horvath, *Spectrochim. Acta, Part B*, 2007, **62**, 1028–1036.
14 O. Dalby, D. Butler and J. W. Birkett, *J. Forensic Sci.*, 2010, **55**, 924–943.
15 K. Bratin, P. T. Kissinger, R. C. Briner and C. S. Bruntlett, *Anal. Chim. Acta*, 1981, **130**, 295–311.
16 K. M. Pun and A. Gallusser, *Forensic Sci. Int.*, 2008, **175**, 179–185.
17 I. R. Lewis, N. W. Daniel and P. R. Griffiths, *Appl. Spectrosc.*, 1997, **51**, 1854–1867.
18 M. E. Morales-Rodríguez, C. W. Van Neste, L. R. Senesac, S. M. Mahajan and T. Thundat, *Sens. Actuators, B*, 2012, **161**, 961–966.
19 Y. A. Gruzdkov, Z. A. Dreger and Y. M. Gupta, *J. Phys. Chem. A*, 2004, **108**, 6216–6221.
20 A. Pallipurath, J. Skelton, P. Ricciardi, S. Bucklow and S. Elliott, *J. Raman Spectrosc.*, 2013, **44**, 866–874.
21 B. M. Wise, N. B. Gallagher, R. Bro, J. M. Shaver, W. Windig and R. S. Koch, *PLS Toolbox 3.5 for Use with MATLAB™*, Eigenvector Research, Inc., Manson, 2004.

